Chapter 5
Heterogenization of Homogeneous Catalysts on Dendrimers

Vital A. Yazerski and Robertus J.M. Klein Gebbink

Abstract The functionalizing of dendrimers with homogeneous catalyst moieties either to the dendrimer periphery or to the dendrimer core yields macromolecular homogeneous catalysts. These polymeric materials are characterized by a high level of molecular integrity and usually retain a comparable activity and selectivity as the parent monomeric catalyst. Moreover, such size-enlarged catalysts can be easily separated from homogeneous reaction mixtures by means of any size-discriminative technique. In this chapter, modern as well as classical examples of dendrimer-heterogenized catalysts will be highlighted in detail with respect to their preparation, properties, and catalytic application with specific emphasis on the role of the dendritic support.

5.1 Introduction

The vivid consumption of limited natural resources in combination with the widespread environmental exposure to human activities is an evident problem of humanity for the twenty-first century. For the modern chemical industry this first of all indicates an urge for the development and application of ultimately atom-efficient and environmental friendly technologies, rather than the simplification and acceleration of already existing chemical processes to economic profits only. A high selectivity is the inherent requirement for any "green" chemical transformation. In turn, a selective process can be realized only on well-defined reaction sites, i.e. catalyst with a molecularly defined structure. Indeed, molecular catalyst design allows for the adjustment of properties of already existing homogeneous catalysts in a predictable manner and allows for the discovery of new ones. However, a major hurdle to implement molecularly defined catalysts, or homogeneous catalysts, in

V.A. Yazerski and R.J.M.K. Gebbink (✉)
Faculty of Science, Debye Institute for Nanomaterials Science, Organic Chemistry & Catalysis, Utrecht University, Padualaan 8, 3584 CH Utrecht, The Netherlands
e-mail: r.j.m.kleingebbink@uu.nl

P. Barbaro and F. Liguori (eds.), *Heterogenized Homogeneous Catalysts for Fine Chemicals Production*, Catalysis by Metal Complexes 33,
DOI 10.1007/978-90-481-3696-4_5,

large-scale operations originates from the solubilized nature of these catalysts and in particular from issues concerning catalyst separation and reuse.

While the immobilization of homogeneous catalysts onto insoluble solid supports such as silica, alumina or cross-linked polymeric materials may solve part of these problems, there are a number of soft spots in this approach that usually suppress their wide application in sustainable technological processes. Molecular catalysts that are heterogenized in this manner typically loose a part of their uniformity in a structural and especially micro-environmental sense, much like typical heterogeneous catalysts, and can no longer be regarded as single site catalysts. These apparent drawbacks along with the possibility of catalyst leaching dramatically influence the overall activity and selectivity of the prepared 'heterogenized' catalysts [1].

The usage of well-known chemical reactions to connect a homogeneous catalyst to a soluble polymeric support has clear benefits over the rather unpredictable immobilization onto insoluble solid supports with their complicated surface morphology. This alternative approach is based on the idea of a significant size enlargement of a molecular catalyst without a differentiation of its molecular and single site properties. The soluble, yet macromolecular nature of the heterogenized catalyst in this case allows for its separation from reaction mixtures using filtration and precipitation techniques and in the end for its recycling for reuse, which includes continuous catalyst operations [2].

Various linear and branched organic polymers have been successfully tested as soluble supports for catalysts, reagents, and substrates [3]. The loading capacity of polymers depends on their branching degree, i.e. branched polymers are potentially superior supports in terms of the amount of supported units per amount of supporting material. For instance, linear monomethoxypoly(ethylene glycol) (MeO-PEG_{5000}) is able to carry only 0.2 mmol catalyst per gram of support, while branched polymers with a branching degree of 50% typically carry at least a tenfold amount of catalyst or even more [4].

Dendrimers are highly symmetrical, hyperbranched organic macromolecules with superb solubility profiles and large sizes and seem ideal supports of choice to arrive at soluble, yet supported homogeneous catalysts. In the case of dendrimers, the degree of branching is close to 100% and, accordingly, a very high theoretical loading can be achieved while maintaining a good solubility.

This chapter focuses on the potential of dendrimers as soluble supports for molecular catalysts. Specifically, we review the different dendrimer families that are used as homogeneous catalyst support, their preparation, the methods for loading and incorporation of catalytic agents onto the dendritic supports, as well as the associated activity. Instead of being comprehensive, we have tried to illustrate the development in the field of dendritic catalysts by presenting selected, yet typical examples.

5.2 Dendrimers

Dendrimers are nanosized, three-dimensional macromolecules that are characterized by a unique tree-like branching structure and compact globular shape in solution (Fig. 5.1) [5–7]. The word "dendrimer" comes from the Greek "δενδρον"/dendron,

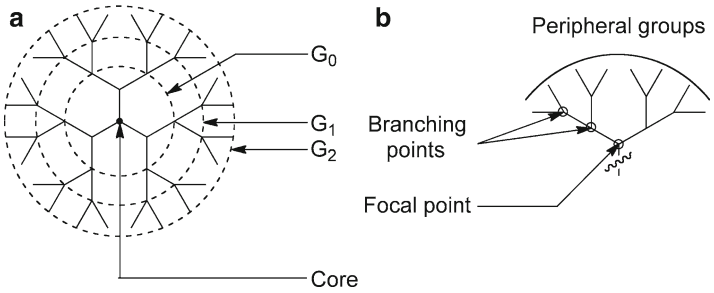

Fig. 5.1 Schematic drawing of a G_2 dendrimer (**a**) and a single dendritic wedge (**b**). Each dashed layer relates to a new generation (G). Peripheral groups form the second generation

meaning "tree" and refers to the singular organization of molecular fragments. Synonymous terms are arborols and cascade molecules.

In 1922 Ingold and Nickolls reported the synthesis of the branched small molecule "methanetetraacetic acid" [8]. This is probably the first example of a directly prepared symmetrically substituted dendritic molecule. Vögtle proposed an iterative methodology toward the synthesis of higher generation dendrimers in 1978 in his paper "Cascade and Nonskid-Chain-like Syntheses of Molecular Cavity Topologies" [9]. In this paper the study and preparation of polymeric branching units with large molecular cavities via repetitive reactions, i.e. exhausted alkylation of amines with acrylonitrile and reduction of newly formed nitriles to primary amines, was described. Only in the middle of 1980s, Tomalia and co-workers reported the first preparation of entire series of dendritic macromolecules, which they called "starburst dendrimers" [10].

Dendrimers are composed of identical "wedges" or dendrons that radiate from a central core in space, forming functional layers of dendritic surfaces. The branching level of dendrons is known as the generation number of a dendrimer (G_n) (Fig. 5.1). This tree-like architecture leads to a predictable geometrical growth of the number of surface groups. Over the past 3 decades, several synthetic strategies were developed to generate multiple dendrimer families with versatile chemical compositions that are useful for a variety of applications in chemistry, biology, and medicine [11].

5.2.1 Properties of Dendrimers

As was described above dendrimers have a well-defined and highly symmetrical molecular structure and a large size. The architectural perfection of such compounds makes them potentially superior supports for homogeneous catalysts, and allows a dispersionless translation of the single-sited nature of molecular catalysts to a heterogenized, dendritic catalyst system with a predefined number of uniform active centers. Hence, this type of dendritic agglomeration of catalytic sites maintains the properties of the single unit at a constant level, while the number of

these units can be tuned in a controllable manner by variation of the nature and architecture of the dendritic support (see also peripheral-functionalized dendrimers, section 5.3.1). The second dendritic strategy of catalyst heterogenization on soluble supports is based on the size-enlargement of a single active site only, via its anchoring to the focal point of a dendron (a single wedge of a dendrimer). This strategy enables the design and synthesis of a defined micro-environment around a catalytic active site (see core-functionalized dendrimers, section 5.3.2).

Both of these concepts toward the immobilization of molecular catalytic sites on dendritic supports are aimed at the creation of continuously active and recyclable catalysts that are easy separable by size-discrimination methods. As for any nanoscaled object, the properties of dendrimes are mostly determined by their surface. This means that the solubility and in particular the hydrophilicity or hydrophobicity of this dendritic material can be adjusted by the mere modification of only the surface terminal groups. This variety and flexibility of dendrimer characteristics is important in the fine-tuning of the retention of dendritic catalysts in membrane reactor technology. In this regard, the heterogenization of molecular catalysts on well-defined soluble supports has become an important research field in homogeneous catalysis. To date several filtration techniques were investigated and optimized at high efficacy for the operation and separation of dendritic catalysts [12–14] (see Chapter 8).

According to these recycling studies, many but not all dendrimer catalysts demonstrate a high stability of their active sites in these processes. In several cases, a predictive additive behavior of the catalytic ensemble of uniform monomolecular units confirms the initial hypothesis about the single-sited nature of the catalysts connected to the dendrimer (neutral dendritic effect). In other cases did the immobilization of a multiple number of catalysts onto a dendrimer provide an alteration of the activity, stability, selectivity etc. of the dendritic catalyst over the (cumulative) properties of its monomeric molecular counter part in either a positive or a negative sense (positive and negative dendritic effects). These findings have pointed out the importance of the choice of the type of dendritic support for particular catalytic reactions. Together, the support and the catalyst connectivity determine the micro-environment of active sites and their isolation or proximity, which in turn is translated on to the catalytic behavior of these sites and explains the observed synergism.

5.2.2 Divergent Dendrimer Synthesis

Divergent dendrimer synthesis represents the assembly of the complete target dendrimer structure from the multivalent core to the periphery by the sequential addition of monomer units (Scheme 5.1) [5].

Starburst dendrimers (the commercial name of PAMAM, polyamidoamine) are the first class of dendrimers that were synthesized using the divergent synthesis strategy [10, 15]. The preparation of each new generation of a PAMAM dendrimer

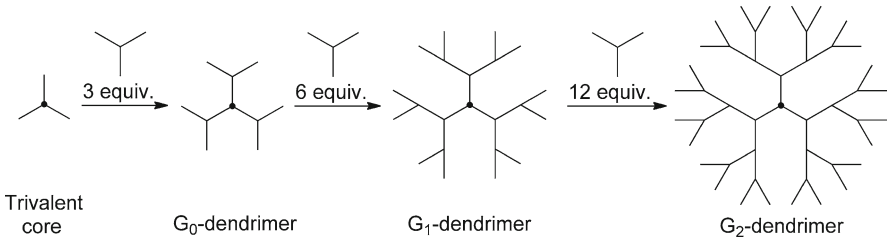

Scheme 5.1 Schematic depiction of the divergent method for the synthesis of dendrimers

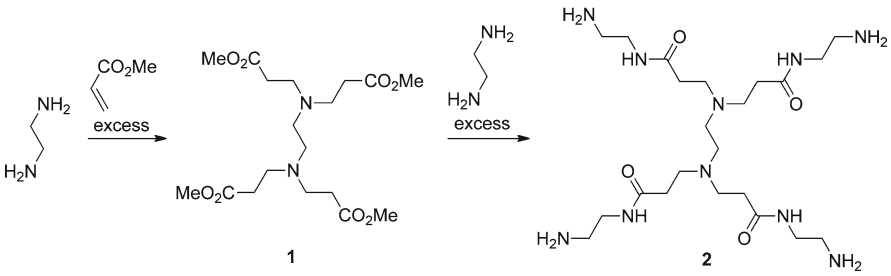

Scheme 5.2 Synthesis of G_0-NH_2 as an example of the divergent synthesis of PAMAM dendrimers

is a two-step process. In the very first step ethylene diamine (EDA) as a tetravalent core is subjected to exhaustive Michael addition of methylacrylate monomers. The resulting aliphatic tetra-ester intermediate **1** subsequently undergoes aminolysis with excess of EDA in the second step to give G_0-PAMAM **2** (Scheme 5.2), which in its own turn serves as a multivalent core for the synthesis of the next generation of PAMAM dendrimer and so on.

Yet, no single chemical process possesses an absolute efficiency due to side reactions and/or the existence of thermodynamic equilibria. In the case of dendrimer synthesis it signifies an inescapable presence of a certain amount of defects in the real dendrimer structure. For instance, amino groups that have not reacted in the Michael addition with methylacrylate, as well as EDA molecules, can participate in a further aminolysis step leading to the formation of intra- or intermolecular links. Even the statistical elimination of whole dendrons is allowed thermodynamically via retro-Michael addition. Large molar excesses of reagents and thorough purification after each step, along with careful thermal control of synthetic processes are used to limit these undesirable side reactions.

The main inherent drawback of any divergent synthesis is a serious reduction of the product yield after a large number of required reaction steps. In the case of dendrimers it also introduces statistically distributed and progressive defects in their structure from generation to generation, that strongly affects the dispersity of the product material.

5.2.3 *Convergent Dendrimer Synthesis*

The convergent schemes in organic synthesis are characterized by usually higher yields of the target product and seem to be superior over divergent schemes in dendrimer assembly [5]. In convergent synthesis, complete dendrimer wedges (dendrons) are prepared prior to their connection to a multivalent core in the last step (Scheme 5.3).

Hawker and Fréchet applied this approach in 1990 for the preparation of poly(aryl benzyl ether) dendrimers. The first step of their dendron synthesis is the regioselective base-catalyzed reaction between 5-(hydroxymethyl)benzene-1,3-diol **3** and bromomethylbenzene [16]. Nucleophilic transformation of the unreacted hydroxymethyl group of the product into the corresponding bromomethyl derivative gives a G_1-dendron **4a** that is able to react with a next portion of 5-(hydroxymethyl) benzene-1,3-diol (Scheme 5.4). This procedure can be repeated until the desired generation is reached, while generating all smaller dendron generations along the line (Fig. 5.2). Finally in the last step of this convergent dendrimer synthesis, G_n-dendrons are attached to 4,4′,4″-(ethane-1,1,1-triyl)triphenol that serves as a trivalent core forming dendrimers **5** (Fig. 5.2).

According to the described strategy, dendrimers up to G_6 were synthesized as almost monodisperse macromolecules (polydispersity index 1.01–1.02). The achieved high purity of the dendrimers is a result of the significant size difference between the target dendrimer and any possible byproduct in the last synthetic step, which facilitates a size-discriminative separation.

In the case of dendrimer synthesis, the last step of the assembly is associated with the reaction of several bulky dendrons with a relatively small core. As a result of the increasing steric hindrance around the dendrimer core after each subsequent introduction of a new wedge, the yields of the target dendrimers are usually moderate or even low. For instance, the chemical yield of the last step of the considered poly(aryl benzyl ether) dendrimers drops from 84% for G_4 to 51% for G_6.

Summarizing, while the divergent approach is convenient for assembling relatively small dendrimers or dendrons, the synthesis of monodisperse, higher generation analogues is an unfeasible task using this approach. The more elaborate convergent approach, on the other hand, is intended for the preparation of dendritic molecules of high purity, but suffers from unsatisfactory yields once applied in the synthesis of higher generation dendrimers due to steric obstacles in the last synthetic step.

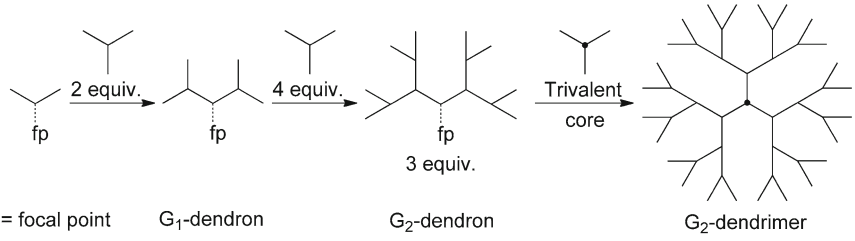

Scheme 5.3 Schematic depiction of the convergent method for the synthesis of dendrimers

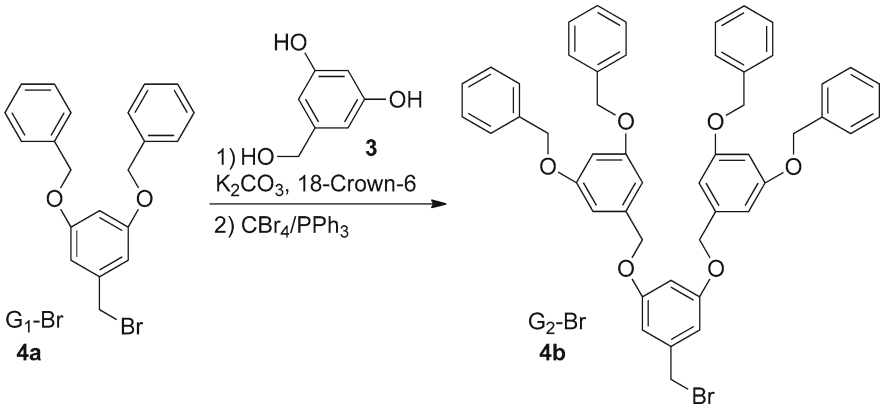

Scheme 5.4 Synthesis of Fréchet-type G_2-dendron

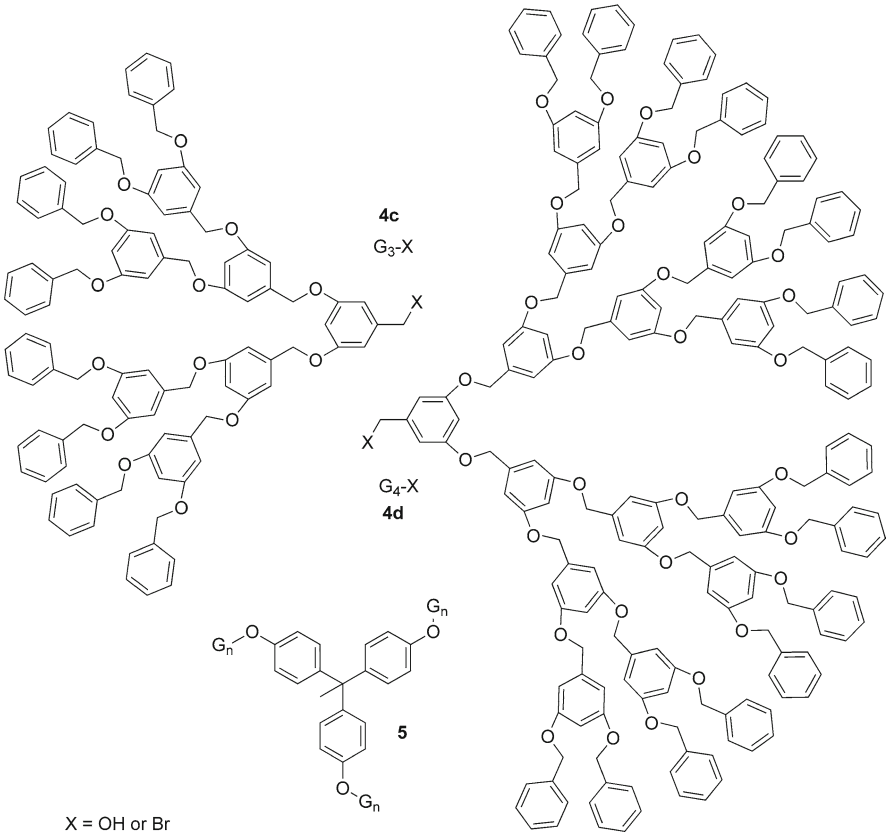

Fig. 5.2 Fréchet dendrons and dendrimer

5.3 Functionalization of Dendrimers

5.3.1 Peripheral-Functionalized Dendrimers

Periphery-modified dendrimers bear numerous catalytic sites at their surface that are directly available to the substrates. In a first approximation any deviation in catalyst behavior after immobilization in this manner is determined by the proximity of elemental sites on a dendrimer. From this point of view the manifestation of a positive dendritic effects can be expected in systems where two or more elemental sites form an active ensemble, i.e. when the kinetic order in catalyst is larger than one. If such agglomeration is undesired and enables side reactions or leads to catalyst deactivation, the prudent choice of support and level of peripheral catalyst loading are crucial to minimize the potential negative impact of peripheral active site accumulation. One of the first published examples of a dendrimer-immobilized catalyst with transition metal active sites was developed and exhaustively studied by the Van Koten group [17]. In particular, NCN-pincer nickel complexes were supported on G_0 and G_1 carbosilane dendrimers.

The selected mononuclear pincer nickel complex demonstrates good results in the regioselective Kharasch addition of polyhalogenoalkanes to terminal alkenes (Scheme 5.5) and is remarkably robust toward self-degradation. The latter stability factor is a prerequisite feature for continuous catalyst usage – the final purpose of immobilization. The highly energetic character of the active high-valent metal species and radicals participating in the Kharasch reaction, furthermore, puts some serious limitations on the nature of the supporting material and asks for a supporting material of very high chemical integrity. In this light carbosilane dendrimers are excellent supports for the chosen catalysts as these are highly resistant toward radical cleavage and have a generally high chemical integrity.

The synthesis of dendritic carbosilane supports is straightforward and includes only two repetitive and quantitative steps: (a) Grignard reaction between a slight excess of freshly prepared allylmagnesium bromide and a chlorosilane compound ($SiCl_4$ or various dendrimers with "$SiCl_n$" end-groups) and (b) hydrosilylation reaction of previously introduced allylic fragments with an appropriate hydrosilane ($HSiCl_3$, $HSiMeCl_2$ or $HSiMe_2Cl$) using a Pt-catalyst (Scheme 5.6).

The immobilization of NCN-pincer nickel complexes on G_0 and G_1 dendrimers was carried out in two steps. First, a special derivative of the prototypical NCN-pincer ligand furnished with a tethered hydroxyl group (OH~NCN) was attached to the carbosilane dendrimer periphery by a stoichiometric alcoholysis reaction with peripheral dimethylsilylchloride groups. The subsequent oxidative addition of

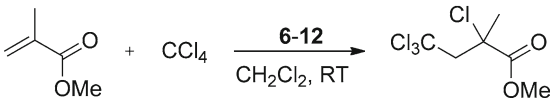

Scheme 5.5 Kharasch addition catalyzed by a metallodendrimer

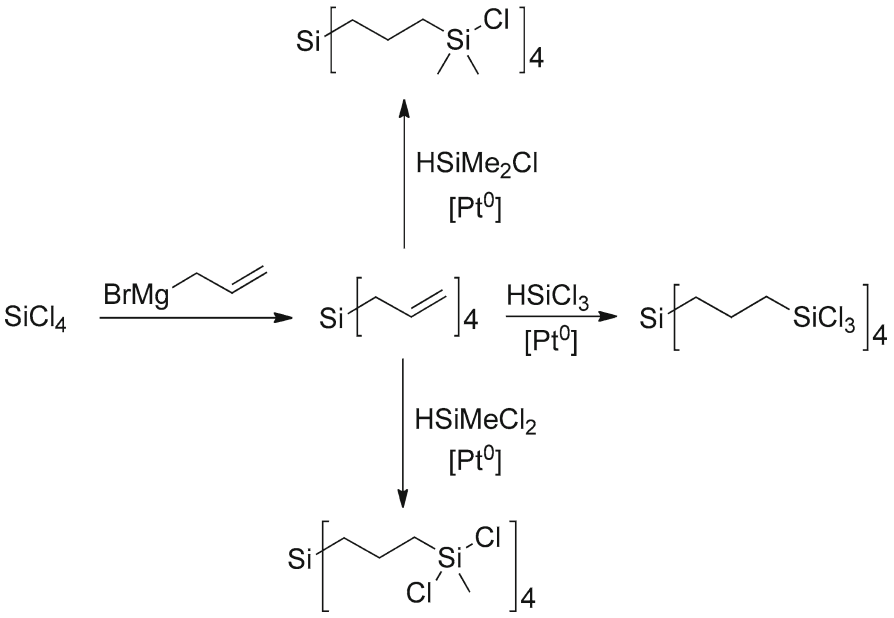

Scheme 5.6 Synthesis of carbosilane dendrimers

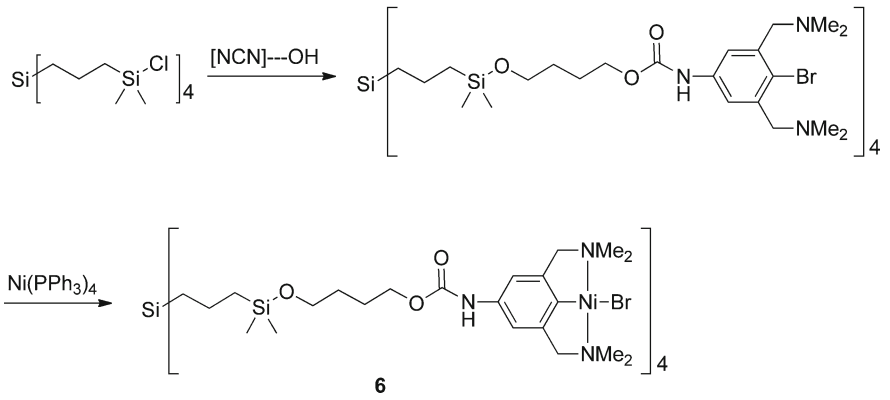

Scheme 5.7 Synthesis of Van Koten's G_0 metallodendrimer

$Ni(PPh_3)_4$ to the immobilized ligand in the second step provided the target metallodendrimers **6** and **7** (Scheme 5.7 and Fig. 5.3).

These Ni-containing dendrimers are active catalysts for the Kharasch reaction much like the monomeric catalyst. The neutral dendritic effect observed in this reaction confirms that a high level of isolation and uniformity of active sites was achieved upon catalyst immobilization. Moreover, the metallodendritic catalysts are nanosized and highly soluble; these physical properties along with the absence of nickel leaching

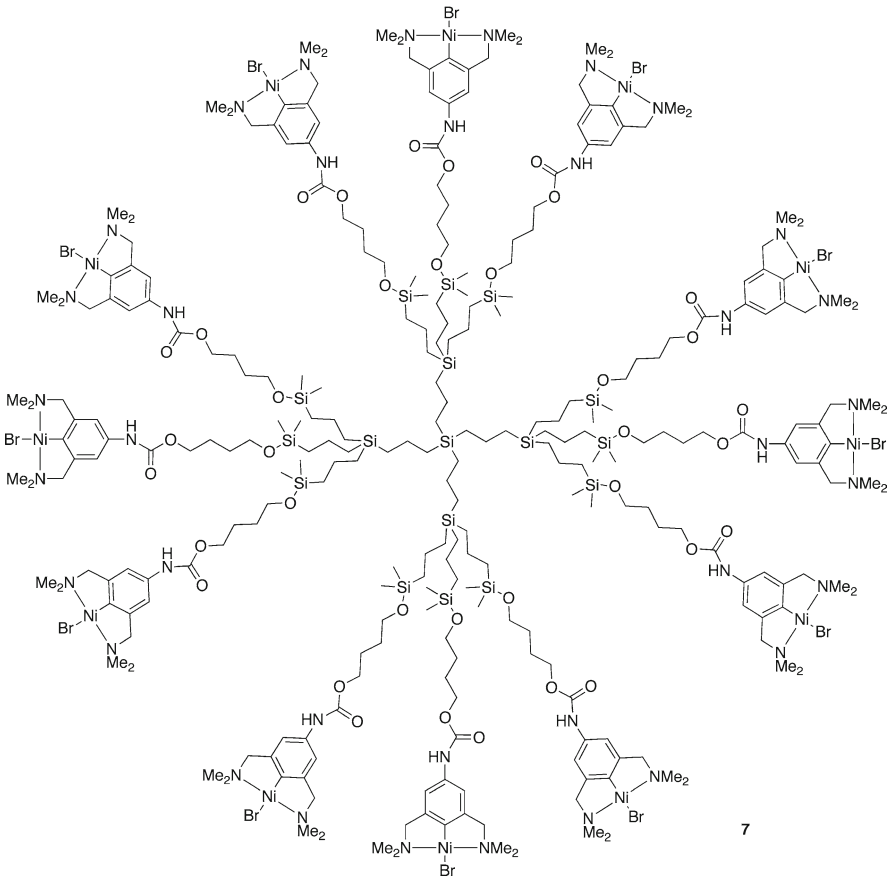

Fig. 5.3 Van Koten's carbosilane G_1 metallodendrimer

make them amenable for homogeneous catalytic applications in nanofiltration membrane reactor set-ups. Overall, this first report on dendrimer-supported catalysts stimulated the development of a new research area in catalysis, i.e. heterogenization of homogeneous catalysts on nanosized, well-defined soluble supports.

Based on these preliminary results, a small library of nickel containing dendrimers (Fig. 5.4) was prepared by Van Koten et al. to estimate the influence of active site proximity – the main factor affecting the catalyst performance in the Kharasch reaction [18, 19]. Also the applicability of the new dendritic catalysts in nanofiltration membrane reactors was comprehensively studied.

The concentration of active sites was tuned through the introduction of different "spacers" in the dendritic framework by changing the substitution patterns at the branching points.

In this study, the metallodendrimers were synthesized starting from a carbosilane dendrimer with terminal $–SiMe_2$-Cl groups via quenching with a para-lithiated

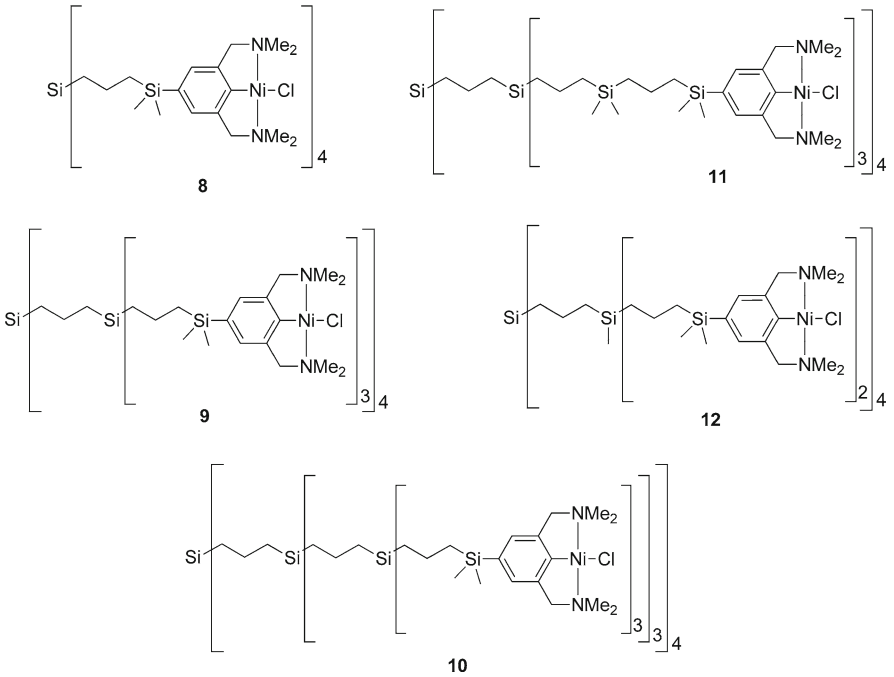

Fig. 5.4 Structure of Van Koten's carbosilane-based catalysts

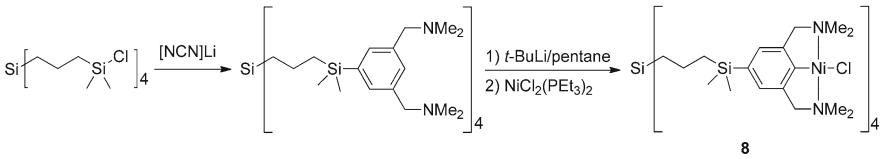

Scheme 5.8 Synthetic pathway for Van Kotens's Ni-based carbosilane metalodendrimers as shown for G_0

NCN-pincer ligand. Subsequent selective deprotonation between the NMe_2-arms of the NCN-pincer ligand with *t*-BuLi and transmetallation with $NiCl_2(PEt_3)_2$ afforded the Ni-containing catalysts (Scheme 5.8). Spectroscopic and elemental analysis indicated that a high level of nickellation (80–90%) was achieved, which corresponds to quite good yields of 90–95% for the last two, synthetically challenging steps.

These dendritic catalysts were examined in the Kharasch addition reaction for which a remarkable degree of variation in activity was observed. The zeroth-generation metallodendrimer G_0-**8** (4 Ni sites) exhibited a similar catalytic activity per Ni-site as its monomeric counterpart. The activity of the first-generation metallodendrimer G_1-**9** (12 Ni sites) was two times less active than G_0-**8** and exhibited significant catalyst deactivation after 1 h (characterized by the formation of a purple precipitate), whereas

the second-generation metallodendrimer G_2-**10** (36 Ni sites) was almost inert. The alternative metallodendrimers G_1-**11** and G_1-**12**, in which the branches are enlarged or the number of peripheral nickel sites is smaller compared to the standard first generation metallodendrimer G_1-**8**, respectively, did not show any sign of catalyst degradation and full substrate conversion was achieved within 22 h.

To explain the observed catalyst deactivation, the authors considered the mechanism of the Ni(II)-catalyzed Kharash addition (Scheme 5.9): in the first step Ni(II) reacts with CCl_4 and forms a Ni(III) species (persistent radical) and a $^{\bullet}CCl_3$ transient radical (initiation of radical chain). The transient radical reacts with a molecule of methylmethacrylate (growth of radical chain) and the newly formed adduct subsequently reduces Ni(III) back to Ni(II), to form the desired addition product (termination of radical chain). In principal, all radical reactions suffer through statistical recombination of active radical species. In this case, the irreversible coupling of two $^{\bullet}CCl_3$ units results in a "half-way" reaction interruption and in the unproductive consumption of CCl_4. The probability of this undesired radical recombination is second order in the transient radical concentration, which makes this process dominant over the Kharash addition (first order in radical concentration) at higher concentrations of $^{\bullet}CCl_3$ species. By extending the spacer length or decreasing the number of peripheral Ni-sites (as is the case for G_1-**11** and G_1-**12**, respectively), the local peripheral radical concentration under the reaction conditions is drastically reduced, along with the rate of catalyst deactivation, to yield metallodendrimers that indeed behave as single-site catalysts in the Kharasch Addition.

Evidently, the non-productive reaction conditions correspond to dendrimers with a high peripheral concentration of active sites (the amount of $^{\bullet}CCl_3$ radicals depends linearly on catalyst concentration) and correlates well with the experimentally

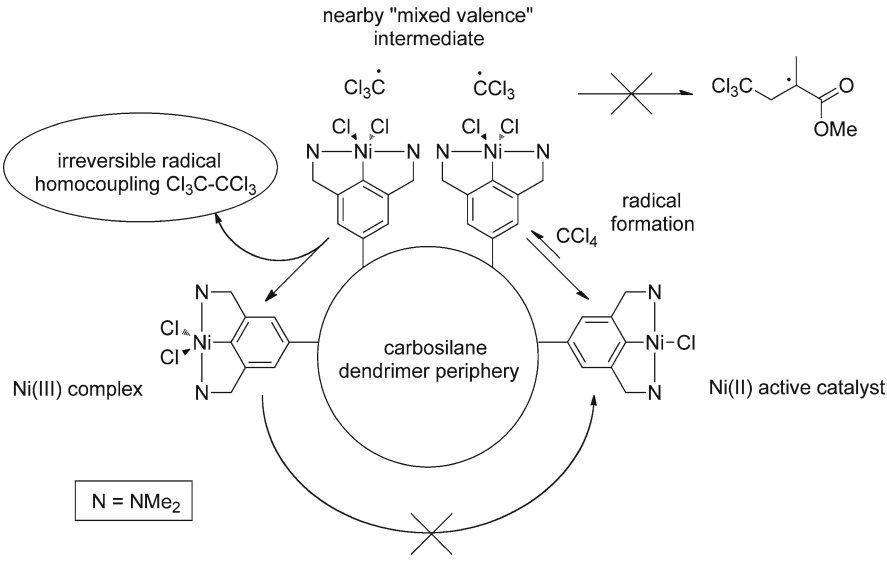

Scheme 5.9 Proposed deactivation pathway for Van Koten's catalysts in the Kharasch addition

observed deactivation trend. These model catalysts, therefore, demonstrate how peripheral catalyst accumulation can lead to negative effects on catalyst activity, and how catalyst activity can be 'restored' by peripheral catalyst 'dilution'.

The pincer-based carbosilane dendrimers G_0-**8** and G_1-**9** were tested for their degree of retention in a membrane reactor equipped with a SelROMPF- 50 nanofiltration membrane. Their retentions are 97.4% for G_0 -**8** and 99.75% for G_1-**9**, indicating that the larger dendrimer (G_1-**9**) is sufficiently retained. Applying the G_1-**9** dendrimer in a continuous flow membrane reactor (CFMR), a significant loss of catalytic activity was observed over 33 h. After continuous membrane reactions (after the reactor volume was replaced 64 times), tests of the retained and filtered fractions indicated that the membrane retained the catalyst at 98.6% (which closely resembled the measured retention found earlier in batch-wise processes for this catalyst). Although this degree of retention leads to some loss of catalytic material in the continuous membrane reactor, it could not solely explain the observed deactivation of G_1-**9** in the reactor. It was, therefore, proposed that the reactive radical intermediates might be interacting with the functional groups of the membrane material and thus influencing the overall reactivity. While the catalyst was effectively retained, it was concluded at that time that new membranes compatible with the reaction conditions used were needed to successfully construct a useful system for continuous operation.

Opposed to the negative dendritic effect observed by Van Koten and co-workers, a positive dendritic effect on the catalytic activity of metallodendrimers was shown in an elegant study by Jacobsen et al. on the hydrolytic kinetic resolution (HKR) of terminal epoxides [20] (Scheme 5.10). This reaction is catalyzed by cobalt(salen) complexes and involves substrate and nucleophile activation by two different catalyst moieties [21]. Theoretically, the proximity of catalyst moieties might result in increased reaction rates in this case due to the bimetallic structure of the transition state, i.e. the second order kinetic dependence on catalyst concentration.

The chiral [Co(II)salen] units were attached to several generations of PAMAM dendrimers through an amide linker via the reaction with activated ester **14** (Scheme 5.11). The obtained crude metallodendrimers were purified by precipitation from a saturated THF solution with hexane and subsequently subjected to size-exclusion chromatography with Sephadex. The final step of the preparation of the active dendritic [Co(III)salen] catalysts was the stoichiometric oxidation of the immobilized [Co(II)salen] groups with molecular iodine in THF.

The activity for HKR of **13** using 0.027 mol% of G_1-PAMAM dendrimer **16** with 8 Co units (Fig. 5.5) was firstly studied. Complete resolution of the racemic epoxide occurred after 20 h, whereas the monomeric catalyst was almost inactive at such low concentrations. This observation can be rationalized by the relatively high local

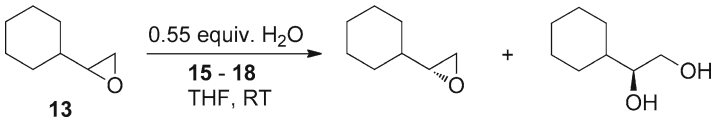

Scheme 5.10 The HKR reaction of epoxide isomers

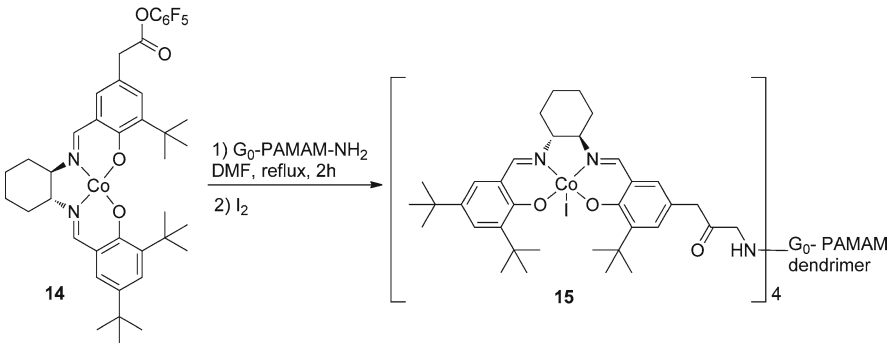

Scheme 5.11 Synthesis of PAMAM-immobilized Co-catalysts for the HKR reaction of terminal epoxides

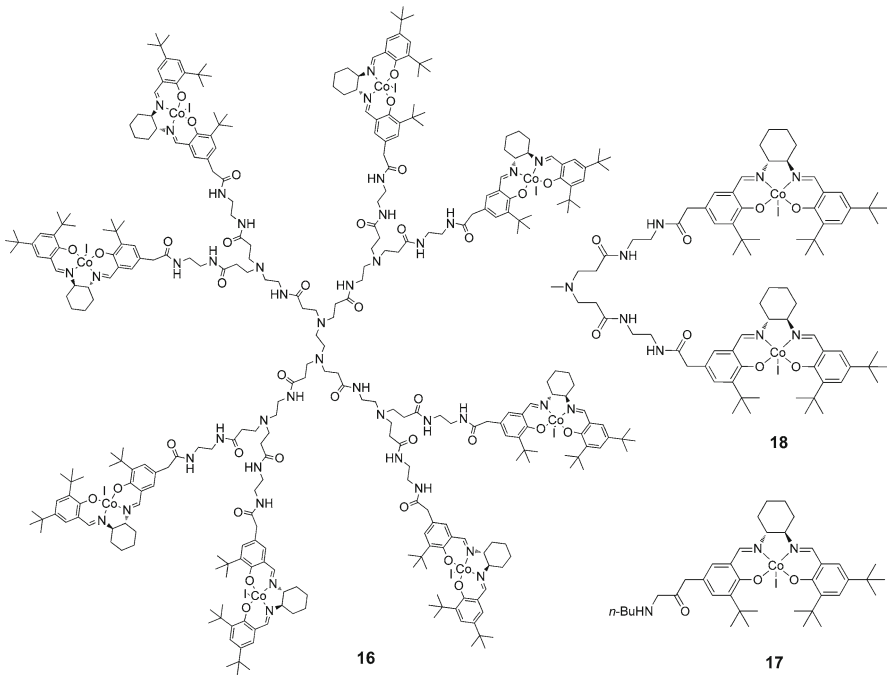

Fig. 5.5 Structures of a G_1 [Co(salen)] dendritic catalyst and model compounds

concentration of active sites connected to one and the same dendrimer. A comparison of the catalytic activity of the monomeric complex and compound **17** also showed a positive electronic influence of the amide linker on the catalyst activity. Nevertheless, this effect is much smaller than the accelerating effect found with the dendritic catalysts, and the close proximity of a second complex moiety is the determinant condition for the increased resolution rate as exemplified by the enhanced resolution rate of the simple bimetallic compound **18**.

The optimal reaction rate was found for G_0-**15** catalyst (Scheme 5.11) where only four salen molecules are conjugated to the dendrimer. It therefore seems that a particular molecular geometry is required for the HKR reaction, which for this series of macromolecules is best obtained in the G_0 dendrimer generation.

Sometimes positive dendritic effects are not only displayed by an increased kinetic behavior of the dendritic catalyst relatively to the monomeric activity of catalyst, but also by the improved characteristics of target products. Such a positive influence of catalyst microenvironment (steric and dielectric tuning of the active site) was observed in an ethylene polymerization study using carbosilane-immobilized bis(imino)pyridyl iron(II) catalysts, carried out by Zheng and coworkers [22]. In this study, zeroth- and first-generation iron metallodendrimers were synthesized in a divergent manner: the ligand **19** furnished with an allylic fragment was anchored to G_0 or G_1 carbosilane dendrimers via a Pt-catalyzed hydrosilylation reaction in 68% and 43% yield, respectively, and was subsequently treated with a stoichiometric amount of $FeCl_2{\cdot}4H_2O$ to furnish the desired metallodendritic compounds (Scheme 5.12 and Fig. 5.6).

The polymerization of ethylene were carried out in toluene under 1 bar pressure of ethylene using the iron metallodendrimers and the parent mononuclear complex as a benchmark catalyst in the presence of activator-modified methylaluminoxane (MMAO). At Al/Fe molar ratios above 1,200, the catalytic activities of the dendritic and mononuclear catalysts are comparable. Yet, both metallodendrimers **20** and **21** yielded polyethylenes (PE) of much higher molecular weights and with higher melting temperatures. At lower Al/Fe ratios, the difference in activity of the immobilized catalysts from the benchmark catalyst becomes significant. For instance at Al/Fe = 500, the iron metallodendrimers are more than two times more active than the corresponding monomolecular complex ($2.5{\cdot}10^3$ kg PE/$mol_{Fe}{\cdot}h{\cdot}bar$ vs. $1.14{\cdot}10^3$ kg PE/$mol_{Fe}{\cdot}h{\cdot}bar$) and produce heavier polymers (M_w~137 kg/mol vs. 62.5 kg/mol) with higher melting temperature (T_m~134°C vs. 128°C).

The noticeable lowering of monomolecular catalyst activity is the predictable response on a decrease of activator (MMAO) content in this reaction. At the same time, the activity of the dendritic catalysts does change slightly over the broad range of Al/Fe ratios that were studies. These results indicate that the catalytic iron

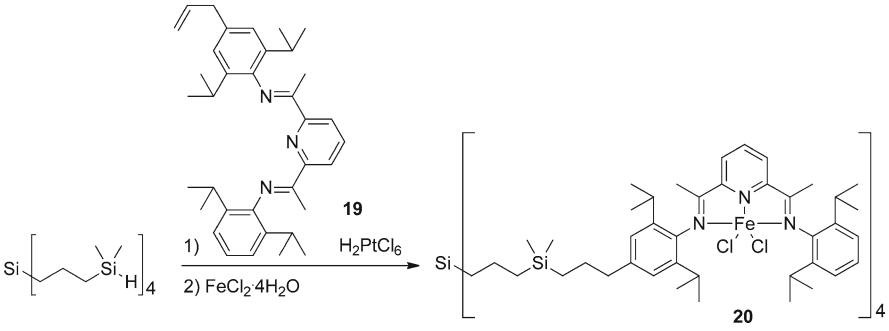

Scheme 5.12 Synthesis of carbosilane-immobilized Fe-catalyst **20** for ethylene polymerization

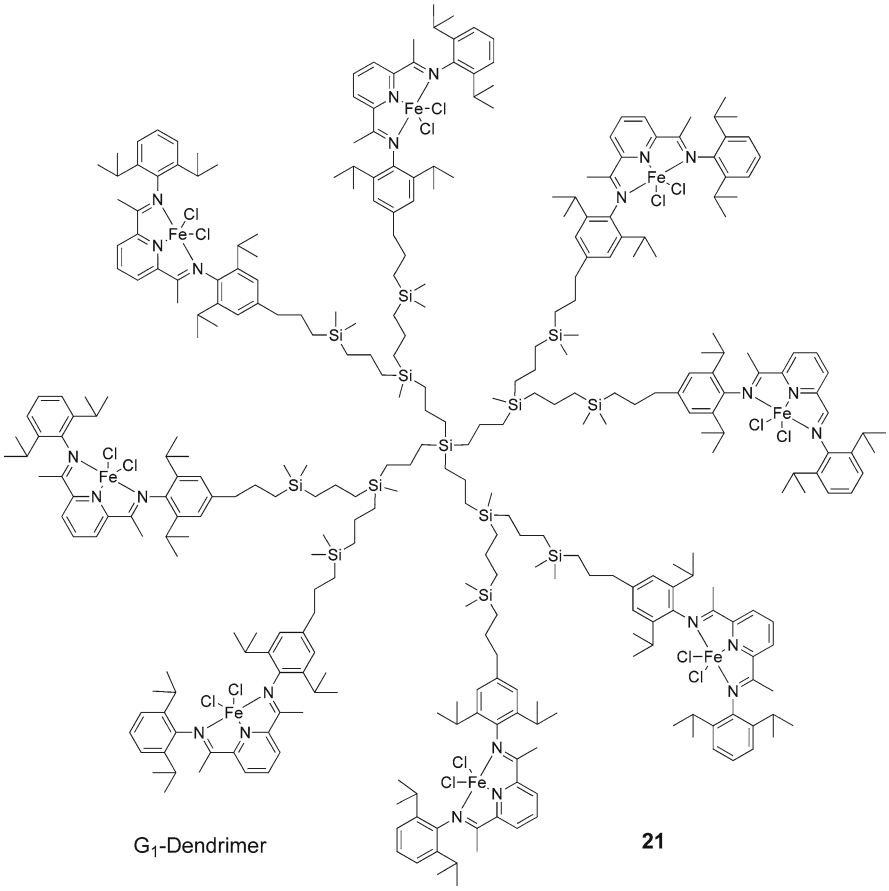

Fig. 5.6 Zheng's G_1 catalyst for ethylene polymerization

site is sterical hindered and therefore stabilized by both dendrimer support moieties as well as by MMAO. Moreover, enforced steric crowding around the active center can decrease the probability of chain transfer reactions during ethylene polymerization to a certain extent and can create favorable conditions for the production of mostly linear PE with higher M_w.

Gade et al. have reported on the immobilization of BINAP ligands on polypropylene imine (PPI) dendrimers (Scheme 5.13) and hyperbranched polymers [23]. Up to the fifth generation dendrimers were successfully synthesized and the corresponding dendritic BINAP-copper(I) complexes were used in the enantioselective hydrosilylation of acetophenone (Scheme 5.14).

The enantioselectivities and activities of the dendritic AMINAP-based catalysts **22** remained almost unchanged upon immobilisation and do not depend on the dendrimer generation. A considerable variation of stereoinduction was observed for G_0–G_5 dendrimers **23** with 4–64 immobilized catalyst units without linker moieties. The first

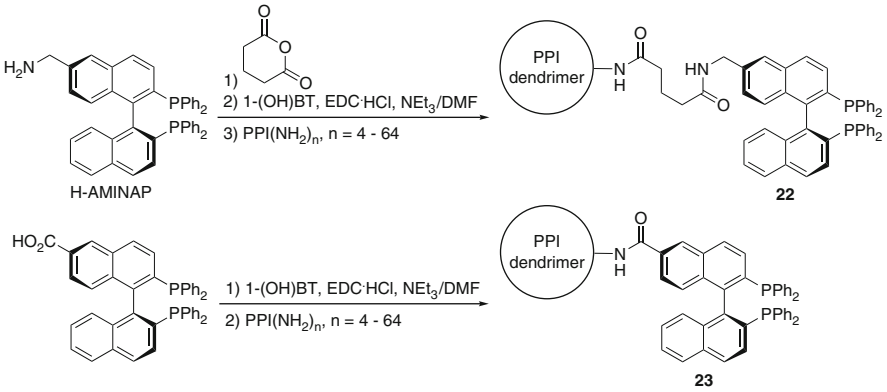

Scheme 5.13 Immobilization of BINAP on PPI dendrimers

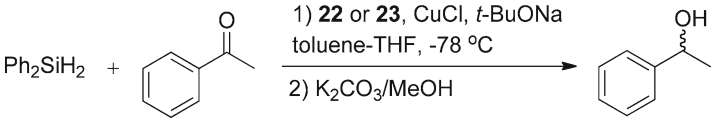

Scheme 5.14 Copper-catalyzed hydrosilylation of acetophenone

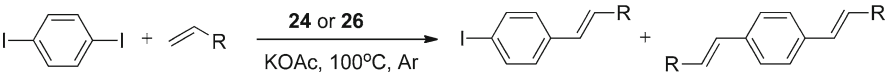

Scheme 5.15 Heck reaction of p-diiodobenzene with olefins using Pd complexes

generation system catalyzed the reaction with a selectivity of only 34% ee and the fifth generation dendrimer reached 90% ee. On the other hand, the reaction time required for complete conversion increased from 24 to 96 h upon going from the mononuclear catalyst to the lower generation dendritic catalysts, whilst decreasing again for the higher generation dendrimers. Decreasing of the CuCl amount from 1 to 0.5 equiv. per BINAP led to an increase in enantioselectivity to 93–95% ee for catalysts **23**.

The G_5-**23** catalyst was removed from the reaction mixture via precipitation and then reused in three successive catalytic runs without loss of activity (TOFs at 50% conversion of 4.7 h^{-1}) or enantioselectivity.

Remarkably, the catalytic characteristics of the hyperbranched polyethyleneimine (PEI)-immobilized BINAP system in this reaction remained unaltered within the range of 9–138 BINAP units per polymer molecule.

Kaneda and co-workers have reported on the control of product selectivity in Pd-catalyzed Heck reactions (Scheme 5.15) and allylic aminations (Scheme 5.16) through the tuning of the dendrimer microenvironment [24].

In this study, the catalysts were assembled by a novel non-covalent approach from decanoyl-terminated polypropylene imine (PPI) dendrimers, (G_2-**24**, G_3 and

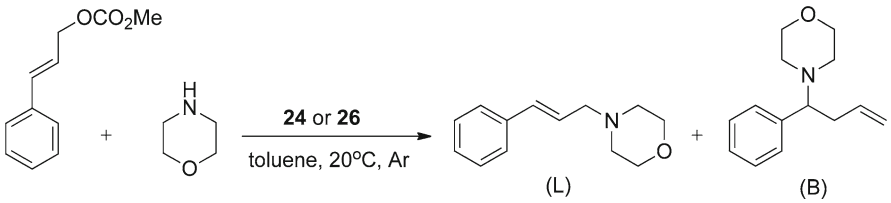

Scheme 5.16 Allylic amination using dendrimer-encapsulated Pd complexes

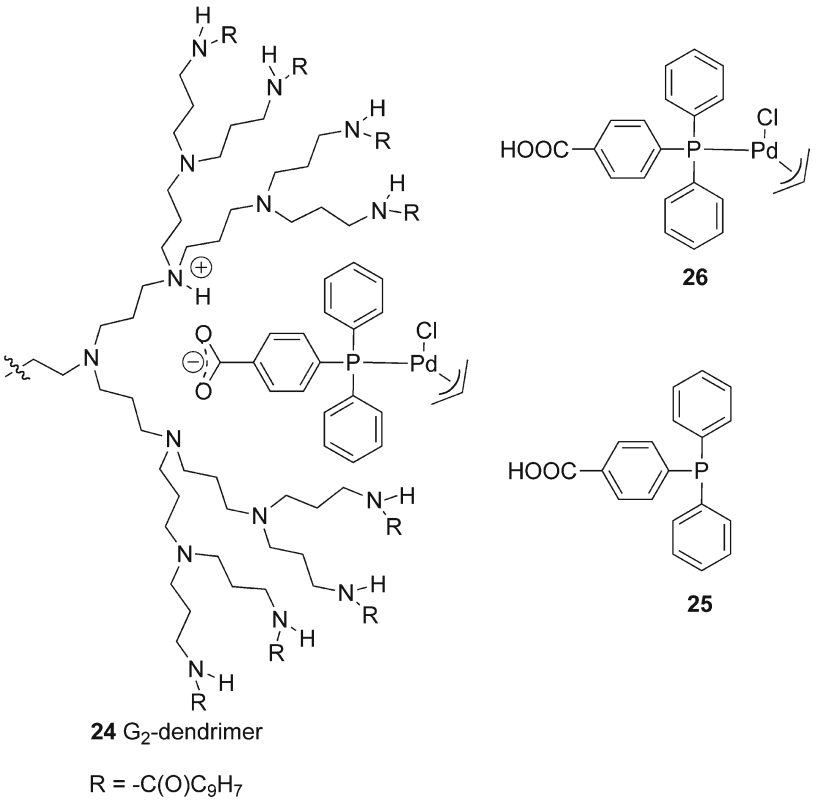

Fig. 5.7 Non-covalent immobilization of anionic Pd-phosphane complexes on PPI dendrimers

G_4) and 4-diphenylphosphinobenzoic acid **25** as the phosphine ligand to locate the Pd complex inside the dendrimers (Fig. 5.7). The formation of ionic bonds between the benzoic acid-derived phosphine ligand and internal tertiary amine moieties of the dendrimer was confirmed by means of ^{31}P, ^{13}C, and ^{1}H-NMR. In this way, the dendrimer encapsulates the Pd complexes and acts as a unique nanoreactor for these versatile catalytic moieties.

In fact, the Heck reaction between iodobenzene and n-butyl acrylate is accelerated with each new generation of dendritic catalyst (Pd/P ratio is 1:1), while in the absence

of the dendrimer no catalytic activity was observed. A similar reaction between 1,4-diiodobenzene and n-butyl acrylate (Scheme 5.15) using the G_4 dendritic catalyst shows a high selectivity toward the mono-Heck coupling product (mono:di=92:8), while the monomeric catalyst **26** possesses a poor selectivity (mono:di=45:55). These experiments strongly suggest that catalysis occurs inside the dendrimers.

In contrast to the case of Heck reactions, the rate of the allylic amination reaction of cinnamyl methyl carbonate with morpholine decreases with increasing dendrimer generation (Scheme 5.16). The same dependence characterizes the rate of olefin hydrogenation by these immobilized catalysts [25]. Probably, the surface overcrowding of the higher-generation dendrimers suppresses the penetration of substrates inside the dendritic nanoreactors. However, such a discrimination effect on the reaction rates was not observed in the above Heck reactions [26].

The predominant formation of linear (L) against branched (B) product in the allylic amination reaction usually occurs in more polar media [27]. The observed L/B rates in the amination reaction carried out with the non-covalently immobilized catalysts in toluene were higher than for the monomolecular catalyst. This fact can be considered as an additional evidence of the influence of the molecular support microenvironment on the active site of the embedded Pd catalyst.

Recycling of the immobilized catalysts derived from decanoyl-terminated dendrimers via precipitation or membrane filtration resulted in some loses of catalytic activity. Modification of the PPI dendrimer with 3,4,5-triethoxybenzoyl chloride instead of decanoyl chloride afforded dendrimers that are amenable for continuous usage and recycling. These dendrimers are well soluble in polar DMF and insoluble in heptane. In the allylic amination of cinnamyl methyl carbonate with piperidine, the thermomorphic phases of DMF and heptane became homogeneous during the reaction at elevated temperature and could be readily separated by cooling the reaction mixtures, where the DMF-phase containing the dendritic material was recycled after decantation from the heptane phase containing the product. This procedure was repeated four times without any catalyst deactivation.

Similar non-covalent approaches to catalyst immobilization on dendrimers were also described by Van Leeuwen [28], Van Koten [29] and Klein Gebbink [30] and have been put forward as facile procedures for dendrimer modification and alteration.

5.3.2 Core-Functionalized Dendrimers

Dendritic effects in core-functionalised dendrimers mainly arise from the site isolation created by the dendritic microenvironment. The steric crowding of a dendritic catalytic core can enhance the stability of the “immobilized” catalyst. At the same time, core immobilization generally suffers from a significantly reduced reaction rate by the catalyst due to the decreased accessibility of the active site. However, in cases where stability determines the overall catalyst activity, dendronization becomes an attractive solution to reach the maximum performance of an expensive catalyst.

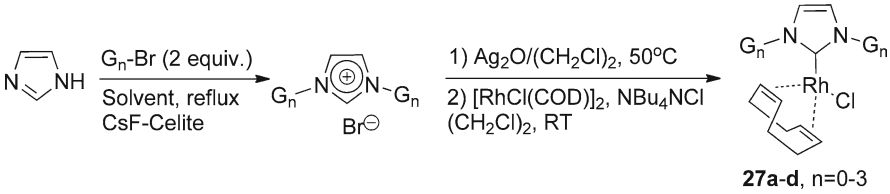

Scheme 5.17 Synthesis of a dendronized Rh-catalyst for the hydrosilylation of ketones

Tsuji et al. applied this concept for the functionalization of rhodium (I) centers with dendritic N-heterocyclic carbenes (NHC) [31]. The straightforward synthesis of these dendritic complexes includes the preparation of G_0–G_3 Fréchet-type dendrons (Scheme 5.4 and Fig. 5.2) and anchoring two equivalents of these to one molecule of imidazole via N-alkylation reactions (Scheme 5.17). Subsequently, silver adducts of the corresponding carbenes were generated from the imidazolium salts by typical treatment with Ag_2O [32]. Finally, these Ag-bis-carbene complexes were subjected to transmetallation with dimeric $[RhCl(COD)]_2$, forming the target metallodendrimers **27a–d**.

These dendritic compounds were employed as catalysts for the hydrosilylation of ketones (acetophenone and cyclohexanone). A positive dendritic effect was observed through an increase in product yield with increasing dendrimer generation. In the hydrosilylation of acetophenone, the product yield was not sensitive toward moderate dilution of the reaction mixture for the G_1–G_3 complexes **27b–d**; however, it dropped from 62% to 44% at 0.41 and 0.29 M substrate concentration in case of the smallest **27a** G_0 metallodendrimer. These observations suggest that the reported dendronized catalysts suffer from mass transfer limitations at the experimental reaction concentrations, except for the G_0-catalyst **27a**.

Cyclic voltammograms of these complexes were recorded in CH_2Cl_2 with *n*-Bu_4NClO_4 as the supporting electrolyte and showed similar irreversible metal-centered oxidation peaks for **27a–c**. In turn, the G_3-**27d** dendrimer does not exhibit a distinguishable oxidation peak, which confirms the essential shielding of the metal core by the bulky dendritic wedges. Based on these observations the authors proposed that for these dendritic Rh-complexes the total turnover number of the monomolecular catalyst increases after the immobilization because the created microenvironment of the metal core suppresses deactivation processes rather than the main catalytic reaction.

In 1999 the group of Van Leeuwen reported the synthesis of a family of core-functionalized carbosilane dendrimers derived from bis(diphenylphosphanyl)ferrocene (dppf) [33]. These macromolecules (G_0–G_2) were assembled from four carbosilane dendrons with an aryl lithium focal point, derived from the corresponding aryl bromide, and ferrocenyl bisphosphonite (Scheme 5.18). Dendrimers with allylsilane moieties at their periphery (R = allyl) were tested as ligands in the palladium-catalyzed allylic alkylation reaction (Scheme 5.19). The complexation of the dendritic dppf ligands with $[PdCl_2(MeCN)_2]$ was monitored by ^{31}P NMR spectroscopy, which confirmed a similar ligand coordination as in monomeric dppf complexes, i.e. one

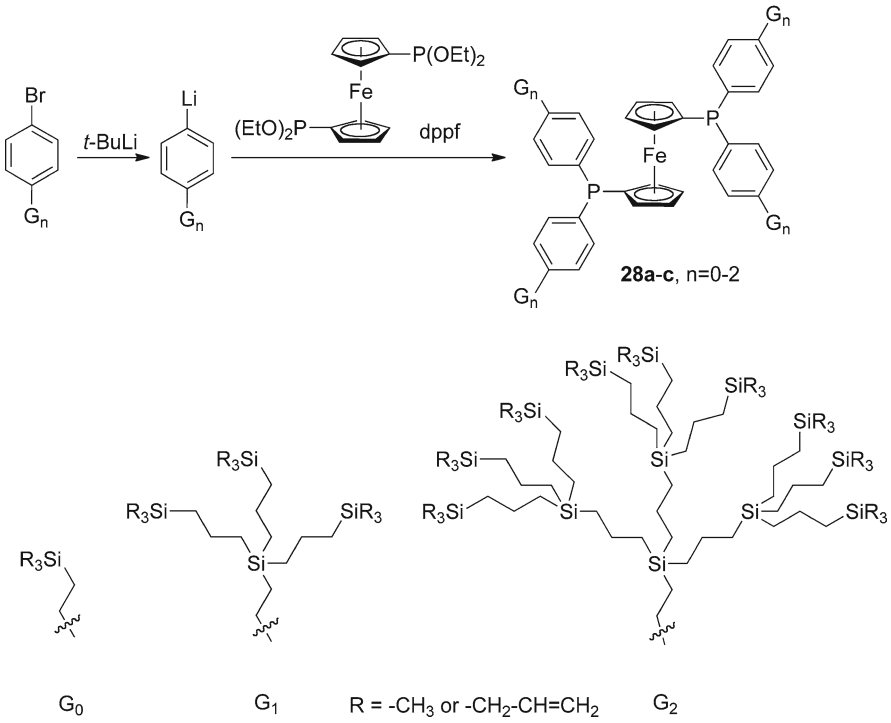

Scheme 5.18 Synthesis of Van Leeuwen's core functionalized ferrocenyl-phosphine carbosilane dendrimers and the structure of their dendrons

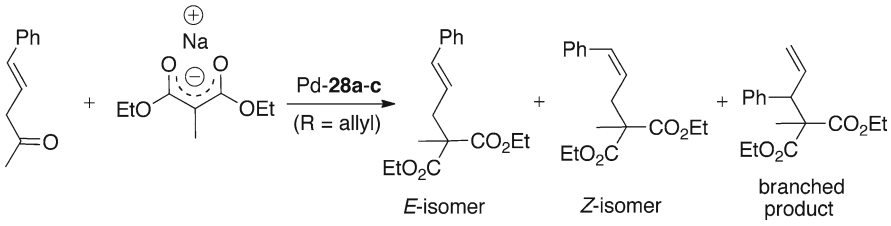

Scheme 5.19 Pd-catalyzed allylic alkylation reaction

bidentate phosphine ligand chelates palladium in a *cis* fashion. In order to perform the catalytic reactions, the active palladium catalysts were generated *in situ*, mixing the selected phosphine ligand and crotylpalladium chloride $[(\eta^3\text{-}C_4H_7)PdCl]_2$ (molar ratio P/Pd = 2:1) in THF followed by addition of the reaction substrates and a base.

Similar substrate conversions were detected for the dendrimers **28a–c** and the monomeric dppf complex, indicating that the peripheral allylic end groups do not participate in the catalytic reaction. The activity and regioselectivity of the alkylation reaction changed with the dendron generation. An increase in the size of the ligand resulted in a decrease in reaction rate, as expected for a restricted

accessibility of the metal centre. Larger dendritic ligands also favoured the formation of the minor, branched product. A change in the local microenvironment caused by the apolar dendritic shell was proposed as one of the possible origins of the modified product selectivity.

The applicability of this type of dendritic catalyst in a CFMR was tested for G_2-**28c**. It was observed that the catalytic activity remained almost constant for up to 8 h of reaction time. Although resulting in an overall lower activity per catalytic center, the location of the catalytic site within the dendritic sphere seems to protect the active species against deactivation via interaction with the membrane or with other metallodendritic species.

Diphosphine core-functionalized dendrimers with a methyl group on the periphery (R = Me, Scheme 5.18) were applied as ligands in the rhodium-catalyzed hydroformylation and hydrogenation of alkenes [34]. For the hydrogenation of dimethyl itaconate (Scheme 5.20), the rhodium catalyst was formed *in situ* via the reaction of $[Rh(nbd)_2]_2(ClO_4)$ (nbd = 2,5- norbornadiene) with the diphosphine dendritic ligand (molar ratio P/Rh = 2). All dendritic dppf-type ligands gave active hydrogenation catalysts with activities similar to the monomeric dppf ligand under the same reaction conditions. In a CFMR, however, the reaction applying the rhodium catalyst of dendrimer G_1-**28b** (R = Me) gave a higher maximum conversion and was more stable over time (77–85% of conversion for 35 reactor volumes) than dppf itself (15–70% of conversion for 35 reactor volumes). The lower conversion observed with dppf was attributed to its lower rate of hydrogenation compared to G_1-**28b** and to leaching of the active Rh–dppf complex.

ICP–AES analysis (induced coupled plasma atomic emission spectroscopy) was performed on the reactor permeate, which showed that the amount of metal leaching is similar to that of the phosphine ligand, i.e. the molar ratio P/Rh is 2 in the permeate. This indicated that the ligand–metal interaction was sufficiently strong under the applied reaction conditions. In addition, measurements on the parent ligands in the membrane reactor showed a retention of 87.5% for dppf and 99.4% for G_1-**28b**, indicating a significantly enhanced retention behavior of the "dendronized" dppf ligands.

The steric crowding of a Mn(III) porphyrin core increases the regioselectivity of the catalyzed olefin epoxidation reaction as was shown by Suslick et al [35]. Within this study a family of oxidatively robust poly(phenylesters) dendrimers was convergently synthesized via anchoring of 8 equiv. of G_1 or G_2 dendrons at the phenolic groups of meso-5,10,15,20-tetrakis(3,5-dihydroxy-phenyl) porphyrinatomanganese-(III) chloride (Mn[T(3′,5′-OHPh)P]Cl) using a DCC coupling reaction in the presence of 4-dimethylaminopyridinium 4-toluenesulfonate (DPTS) as the catalyst (Scheme 5.21).

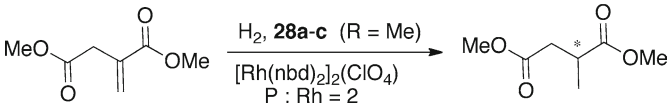

Scheme 5.20 Rh-catalyzed asymmetric hydrogenation

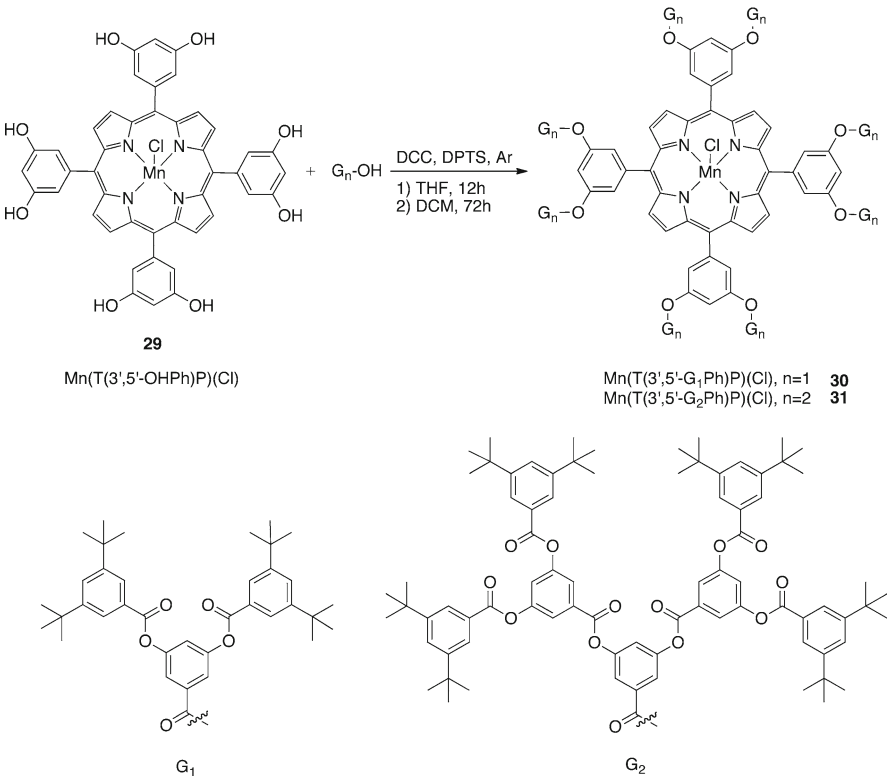

Scheme 5.21 Synthesis of Mn(III) complexes of dendrimer-porphyrins and the molecular structure of the monodendrons

The purity and integrity of the obtained compounds were confirmed by HPLC and MALDI-TOF MS data. The mass spectra contain exclusively the molecular ion peak $[M\text{-}Cl]^+$ (m/z = 5,344.0 (calcd. [M-Cl] 5,346.2) and 10,980 (calcd. 10,985)), respectively for the G_1-**30** and G_2-**31** metallodendrimers. In the latter, two minor peaks were observed at m/z = 9,724 and 8,462, which is possibly due to the successive loss of one and two G_2 dendrons from the parent molecular ion (calcd. m/z = 9,694 and 8,437, respectively).

The catalytic epoxidation reactions using these dendronized Mn-porphyrins were carried out under oxidant limiting conditions using iodosylbenzene as the oxygen donor. In the epoxidation of nonconjugated dienes and 1:1 mixtures of linear and cyclic alkenes under competitive conditions, the dendritic catalysts selectively epoxidize the less hindered double bond and this regioselectivity increases with increasing dendrimer generation.

Sterically demanding dendrons tethered to the meta-positions of meso-tetraphenyl porphyrin (TPP), extremely limit the access to the catalytic metal core. This is the clue to the origin of discrimination of more hindered double bonds in a substrate

with increasing dendrimer generation, i.e. the preferred oxidation of sterically available double bonds.

A competition experiment between cyclohexene and cyclooctene also indicated the presence of a certain positive electronic effect of the dendron substituents. While the G_1-**30** outperforms the parent molecular catalyst Mn(TPP)(Cl) in selectivity more than twice, the selectivity of the G_2-**31** metallodendrimer equals that of the G_1-**30** metallodendrimer. Interestingly, the "immobilization" of the manganese porphyrin complex does not influence the overall catalyst activity. The turnover frequency values obtained for dendronized complexes (2-4 s^{-1}) are similar to that of Mn(TPP)(Cl) (3–4 s^{-1}). Moreover, a fair resistance toward selfoxidation during catalysis was observed for the dendritic metalloporphyrins. Even after 1,000 turnovers (of oxidant) less than 10% degradation occurred (according to UV–Vis data).

Recently, the group of Tsuji has designed novel NHC ligands that are furnished with tetraethylene glycol (TEG) and *n*-C_{12} alkyl chains (Fig. 5.8) [36]. Both of these compounds were tested in the palladium-catalyzed Suzuki–Miyaura coupling of aryl bromides. It was found the TEG moieties of **32a** considerably enhance the catalytic activity in this reaction, whereas the *n*-C_{12} alkyl chains of **32b** do not influence the catalysis. The observed positive dendritic effect arises from the stabilization of the active centers by changes in the dielectric properties of their microenvironment through the TEG moieties. However, these NHC ligands failed to catalyze more challenging reactions, e.g. the activation of the less reactive aryl chlorides for Pd-mediated cross-coupling reactions.

Site-isolation may also lead to the formation of low-coordination number metal complexes, which in turn may have enhanced catalytic properties [37]. Two independent examples that illustrate this concept were recently reported by the groups of Tsuji [38] and Klein Gebbink [39].

On the base of bulky phosphane analogues of their NHC ligands, highly active catalytic systems were developed by Tsuji et al. for the Suzuki-Miyaura coupling of aryl chlorides [38]. In particular, a family of new triarylphosphanes in which the TEG (**33a**, **34a**) or *n*-C_{12} (**33b**, **34b**) moieties are arranged radially around the phosphanes was designed and prepared (Fig. 5.8). The high yielding and straightforward synthesis of these ligands includes the reaction of tri(4-hydroxyphenyl) phosphane oxide with the corresponding benzyl chlorides followed the reduction of the phosphane oxides with $PhSiH_3$ (Scheme 5.22). Amongst these dendritic phosphanes, the second-generation dendritic derivative with TEG chains is distinctly effective as a ligand and provides a highly active Pd catalyst system for the Suzuki–Miyaura cross-coupling reactions.

The dendrimers were tested as ligands in the Suzuki–Miyaura coupling of 4-chlorotoluene with phenylboronic acid (2 equiv.) in combination with $PdCl_2(PhCN)_2$ (0.1 mol% Pd, 0.2 mol% ligand) with K_2CO_3 in THF at 60°C (Scheme 5.23). While the application of **33a** with the TEG moieties afforded 4-phenyltoluene in 36% yield, the next generation dendrimer **34a** afforded the product in 93% yield (a positive dendritic effect). In contrast, phosphane dendrimers with *n*-C_{12} alkyl chains (**33b**, **34b**) do not exhibit any dendritic effect [40] being almost unactive catalysts for this coupling, which parallels the use of the parent ligand PPh_3 in this reaction.

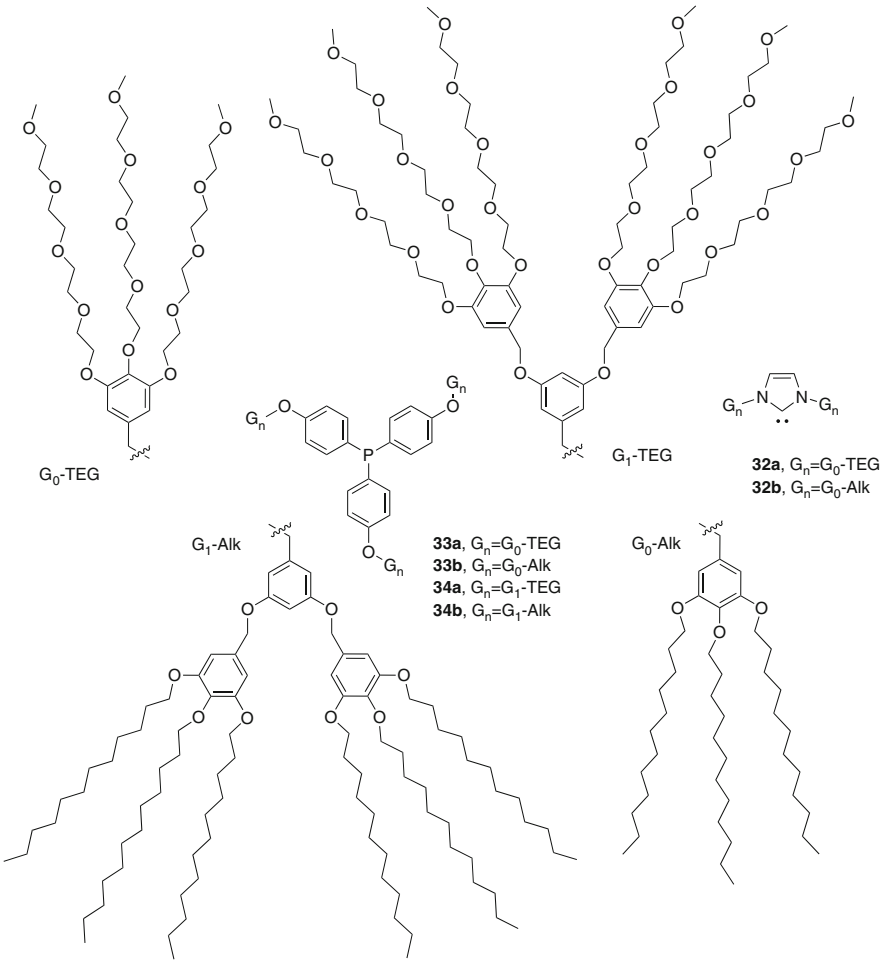

Fig. 5.8 *N*-Heterocyclic carbene and phosphane ligands bearing tetraethylene glycol or n-C_{12} moieties

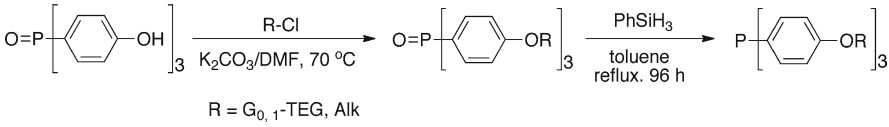

Scheme 5.22 Synthesis of phospane dendrimers

The efficiency of **34a** as the ligand essentially depends on the type of solvent and base used in the reaction. For instance, the highest yield of cross-coupling products was achieved in THF. In the solvents DME, DMF, 2-propanol, and water the products were obtained in only low to moderate yields and 1,4-dioxane and toluene, very common solvents for the Suzuki–Miyaura coupling reaction, were not suitable for the present system

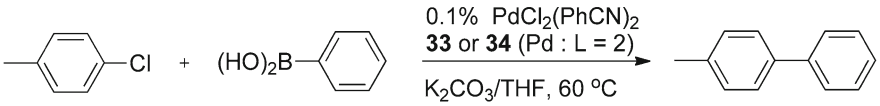

Scheme 5.23 Pd-catalyzed Suzuki-Miyaura reaction in the presence of phosphane dendrimers

at all. Among the bases, potassium and rubidium salts are more favorable for catalysis; in the presence of sodium, cesium and lithium salts only low yields were obtained.

The special role of the dendritic TEG moieties of **34a** in catalysis was confirmed by several control experiments. Under identical catalytic conditions a mixture of PPh_3 and tetraethylene glycol dimethyl ether (molar ratio = 1:18) instead of ligand **34a** did not afford any product.

Because dendrimers are known to stabilize nanoparticles [41], a mercury test [42] was performed in order to examine the possibility of zero-valent nanoparticles to act as active catalyst species. In this experiment the cross-coupling product was obtained in a significant yield (55%), even in the presence of 25 mol% mercury. The authors, therefore, concluded that it is unlikely that nanoparticles act as the active catalyst species in this system.

Interestingly, both **34a** with TEG moieties and its alkyl analogue **34b** possess identical basicities based on the ^{31}P-Se coupling constants [43] of the corresponding phosphane selenides ($^1J_{P,Se}$ = 715 Hz). This value is close to the one for PPh_3 ($J_{P,Se}$ = 730 Hz) and much larger than P(*t*-Bu)$_3$ ($J_{P,Se}$ = 686 Hz) and PCy_3 ($J_{P,Se}$ = 674 Hz), which are known to be strong π-bases.

From a steric point of view, bulky phosphanes facilitate the formation of coordinatively unsaturated and highly reactive catalyst species that can participate in the oxidative addition step of strong aryl–Cl bonds. In an experiment with a double amount of the phosphane ligand **34a** (molar ratio P/Pd = 4:1), the initial reaction rate decreased to one-thirtieth of the rate for a normal amount of phosphane (molar ratio P/Pd = 2:1). This observation is in line with the assumption shown above, as the existence of unsaturated complexes becomes more unfavorable at higher ligand concentration.

The group of Klein Gebbink designed a related type of dendritic phospine ligands "Dendriphos" (Fig. 5.9) [39, 44, 45]. These behave as very bulky phosphine ligands and, hence, can stabilize coordinatively unsaturated and catalytically active Pd(0) species that are crucial for the activation of relatively inert substrates such as aryl chlorides in cross-coupling reactions.

Dendriphos ligands were successfully employed in the palladium-catalyzed Suzuki–Miyaura cross-coupling of aryl halides. While this reaction in case of aryl bromides occurs pretty smoothly and without any visible dendritic effect, the behavior of aryl chlorides is quite interesting and was investigated in detail.

Following a standard alkylation procedure the Fréchet-type G_0-G_2 dendrons were tethered to the triphenylphosphine core furnished with six dimethylamino groups. All synthesized hexacationic Dendriphos macromolecules were used as ligands in the palladium-catalyzed Suzuki–Miyaura cross-coupling of 4-nitrochlorobenzene and phenylboronic acid in combination with $Pd_2(dba)_3{\cdot}CHCl_3$ (0.1 mol% Pd, 0.25 mol%

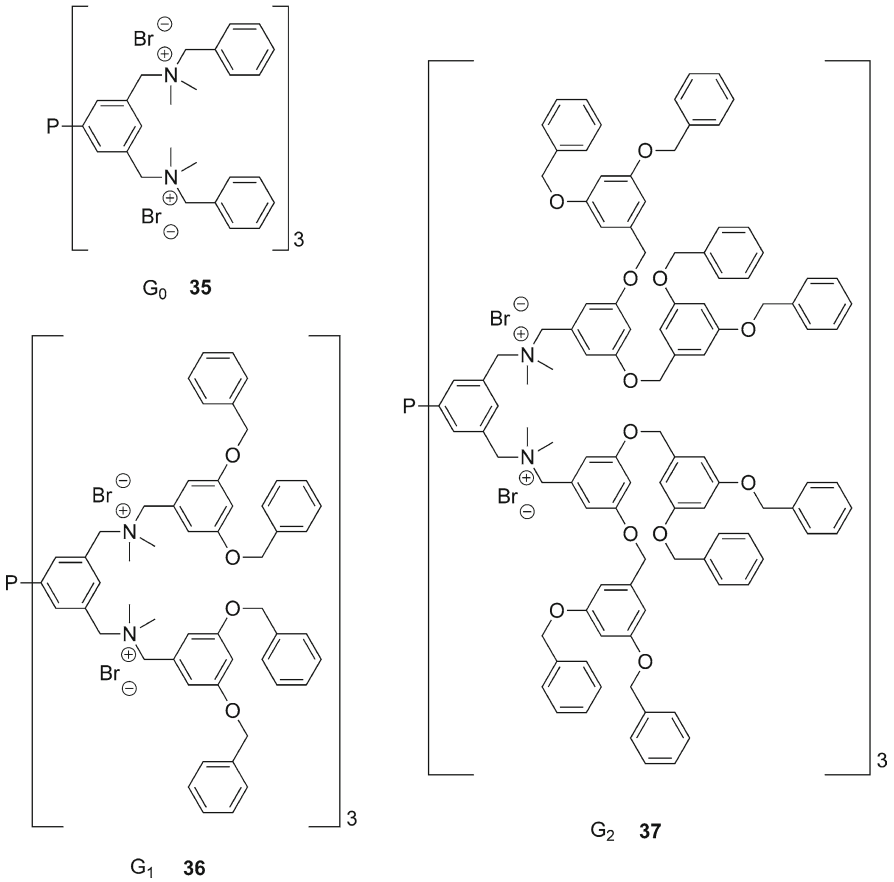

Fig. 5.9 Dendriphos ligands for Suzuki-Miyamura couplings

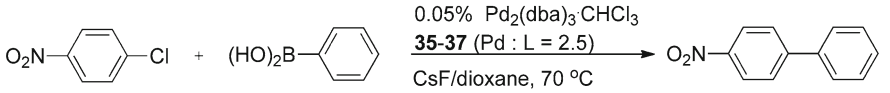

Scheme 5.24 Pd-catalyzed Suzuki-Miyaura reaction in the presence of Dendriphos ligands

ligand) and a base (CsF) in dioxane at 70 °C (optimized conditions) (Scheme 5.24). The kinetic data of these reactions confirmed a strong positive dendritic effect. In the presence of the most active G_2-**37** Dendriphos ligand, the yield of 4-nitrobiphenyl was 80% after 3 h, while in case of G_1-**36** and G_0-**35** phosphanes about 40% and 30% yields, respectively, were determined. However, at 95 °C thermal decomposition of G_1-**36** and G_2-**37** ligands was observed, while the activity of G_0 increased.

Several experiments were carried out to reveal the nature of the active species in these reactions. Blank reactions with PPh_3 in combination with a bis(tetra-alkyl)ammonium dendron did not produce a serious amount of cross-products. This observation confirms the special role of the Dendriphos architecture in the activation of aryl halides and the acceleration of cross-coupling reactions with increasing dendrimer generation.

Poly(4-vinylpyridine) (PVPy) is known to act as a selective trap for homogeneous, ligandless Pd(0) species [46]. Addition of PVPy to the catalytic system Pd_2dba_3 $CHCl_3$/**35** did not have any effect on the catalytic activity. This is a strong indication that, in the present system, the observed activity cannot be attributed to ligandless Pd(0) species, but to a homogeneous Pd-Dendriphos complex of the type $Pd(0)L_n$.

Rothenberg et al. reported on the immobilization of Ru(II) complex with (*S,S*)-*N*-arenesulfonyl-1,2-diphenylethylenediamine ligands (Ts-DPEN) on a third-generation Fréchet-type dendron [14]. Previously, this complex was developed by Noyori and Ikariya as an asymmetric transfer hydrogenation catalyst [47]. The core functionalized dendritic ligand **40** was synthesized by condensing the Boc-protected amino derivative of (*S,S*)-DPEN **39** with the G_3-**38** polyether dendron (Scheme 5.25). Subsequently the Boc group was removed and the dendritic ruthenium complex was prepared by mixing the dendrimer ligand with $(RuCl_2(cymene))_2$ at 25 °C in THF.

This metallodendritic catalyst was used in the asymmetric transfer hydrogenation of acetophenone with *i*PrOH in the presence of *i*PrOK as a base (Scheme 5.26).

After 48 h a substrate conversion of 65% was achieved, yielding predominantly (*S*)-1-phenylethanol (95% ee). Neither the reverse reaction nor significant catalyst deactivation was observed.

After these encouraging results the catalyst was tested in a specially designed ceramic membrane reactor. This reactor has a cylindrical shape (15 × 7 mm) and walls made of a thin nanoporous γ-alumina layer, covering a macroporous α-alumina

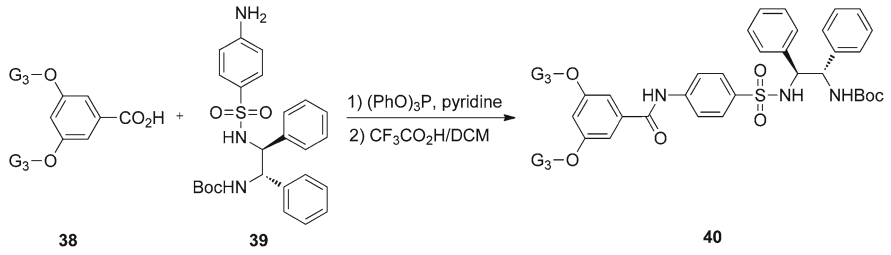

Scheme 5.25 Synthesis of a Ts-DPEN ligand with a third generation Fréchet dendron

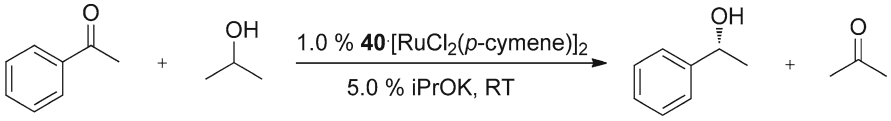

Scheme 5.26 Asymmetric transfer hydrogenation in the presence of a dendronized Ru-catalyst

membrane [13]. The reactor is closed with teflon caps on both sides. In this way, a macromolecular dendritic catalyst can be placed inside this small reactor and subsequently introduced into the reaction mixture. At the end of the reaction, catalysts retained inside of the cap can be easily separated, purified from the reaction mixture, and recycled. The molecular-weight cutoff of the γ-alumina layer is 1,000 Da. The reaction permeate was analyzed via inductively coupled plasma mass spectrometry (ICP-MS) analysis and it was found that less than 0.3% of the Ru leached into the permeate solution after 48 h.

A series of control experiments were run to determine the background reaction level. No reaction was observed in the absence of catalyst or when only the dendritic ligand was present. Reactions run with the Ru precursor salt, the Ru non-dendritic complex, and the Ru–dendrimer complex are characterized by similar conversion values, however only the latter two catalysts act in an enantioselective manner (93–95% ee in both cases). Finally, the same catalyst was used in two subsequent runs and gave practically identical conversions, selectivities, and reaction rates. These data clearly confirm that the Ru catalyst retains inside the membrane reactor in the form of the dendrimer-supported complex.

Related 'cat-in-a-cup' or 'tea bag' approaches have been reported by Van Koten [48] and by Vogt [49].

5.4 Conclusions and Outlook

The application of homogeneous catalysts undoubtedly has a superior potential over heterogeneous catalysts in synthetic organic operations where both reaction selectivities in terms of the regio- and stereo-selectivity of product formation, as well as a total predictability of the overall process are mandatory. Moreover, molecular catalysts possess an incomparable higher activity and occur almost without additional thermal activation, which allows for shorter operation times and decreases the overall energy costs of production. These inherent irreprehensible properties of homogeneous catalysts lay a foundation for a "green" chemical technology using environmentally friendly processes. However, homogeneous catalysts also have one, albeit extremely undesirable consequence of their molecular nature: the self-contamination of reaction products, which are often not easily separated from even tiny amounts of metal-containing catalysts. Consequently, the molecular nature of homogeneous catalysts also imparts the ability to regenerate and recycle either the ligand or metal component, and ultimately both components of homogeneous catalysts.

Elaborated approaches for homogeneous catalyst separation from product streams based on size-discrimination concepts have found considerable attention in recent years and allow for the previously unfeasible separation of molecular components within one phase according to their size. According to these approaches, the artificial size-extension of catalyst molecules might be

applied to facilitate their discrimination, i.e. separation, among reaction product molecules. The task of homogeneous catalyst 'immobilization' via molecular size enlargement brings new challenges to the development of homogeneous catalyst. These challenges mainly deal with the maintenance of particular molecular catalyst properties like activity and selectivity at the same level as those of the 'non-immobilized' parent catalysts.

Within this chapter we have combined a brief historical description with selected recent examples of the contemporary scientific progress in the relatively young and developing field of homogeneous catalyst heterogenization on dendritic supports, as a most promising way toward the flawless transfer of molecular catalyst properties on the macromolecular level. We have discussed the main problems that may be associated with this approach, next to its anticipated and appreciable benefits, and by doing so have tried to highlight the unique features of the dendrimer supports.

Although the field has gone through a rapid progression phase, several hurdles remain for the commercialized use of dendritic and dendronized molecular catalysts. Clearly, the specialty, i.e. expensive, nature of dendrimer materials needs to be addressed. While alternative molecular supports such as hyper-branched polymers have been put forward, the development of novel high-definition dendrimer and dendron classes needs further attention. In addition, the further technological development of practical filtration set-ups, which has been advocated since the early days of the field, has yet to result in applicable and affordable 'molecular' filtration protocols. In our opinion, these aspects are prerequisites for the development of economically viable synthesis protocols based on size-enlarged homogeneous catalysts.

References

1. Frenzel T, Solodenko W, Kirschning A (2003) Solid-phase bound catalysts: properties and applications. In: Buchmeiser MR (ed) Polymeric materials in organic synthesis and catalysis. Wiley, Weinheim
2. Berger A, Klein Gebbink RJM, van Koten G (2006) Top Organomet Chem 20:1–38
3. Dickerson TJ, Reed NN, Janda KD (2002) Chem Rev 102:3325–3344
4. Haag R, Roller S (2003) Dendritic polymers as high-loading supports for organic synthesis and catalysis. In: Buchmeiser MR (ed) Polymeric materials in organic synthesis and catalysis. Wiley, Weinheim
5. Newkome GR, Moorefield CN, Vögtle F (2001) Dendrimers and dendrons: concepts, syntheses, applications. Wiley, Weinheim
6. Vögtle F, Richardt G, Werner N (2009) Dendrimer chemistry: concepts, syntheses, properties applications. Wiley, Weinheim
7. Bosman AW, Janssen HM, Meijer EW (1999) Chem Rev 99:1665–1688
8. Ingold CK, Nickolls LC (1922) J Chem Soc 121:1638–1648
9. Buhleier E, Wehner W, Vogtle F (1978) Synthesis 1978:155–158
10. Tomalia DA, Baker H, Dewald J et al (1985) Polymer J 17:117–132
11. (a) Gillies ER, Frechet JM (2005) J Drug Discovery Today 10:35–43; (b) Boas U, Heegaard PMH (2004) Chem Soc Rev 33:35–43; (c) Chase PA, Klein Gebbink RJM, van Koten G (2004)

J Organomet Chem 689:4016–4054; (d) Peng X, Pan Q, Rempel GL (2008) Chem Soc Rev 37:1619–1628; (e) Helms B, Fréchet JMJ (2006) Adv Synth Cat 348:1125–1148
12. (a) Dijkstra HP, van Klink GPM, van Koten G (2002) Acc Chem Res 35:798–810; (b) Vankelecom IFG (2002) Chem Rev 102:3779–3810
13. (a) Benes N, Nijmeijer A, Verweij H (2000) Microporous silica membranes. In: Kanellopoulos NK (ed) Recent advances in gas separation by microporous ceramic membranes. Elsevier, Amsterdam; (b) van Gestel T, Vandecasteele C, Buekenhoudt A et al (2003) J Membr Sci 214:21–29
14. Gaikwad AV, Boffa V, ten Elshof JE et al (2008) Angew Chem Int Ed 47:5407–5410
15. Tomalia DA, Naylor AM, Goddard WA III (1990) Angew Chem Int Ed 29:138–175
16. Hawker CJ, Frechet JMJ (1990) J Am Chem Soc 112:7638–7647
17. Knapen JWJ, van der Made AW, de Wilde JC et al (1994) Nature 372:659–663
18. Kleij AW, Gossage RA, Jastrzebski JTBH et al (2000) Angew Chem Int Ed 39:176–178
19. Kleij AW, Gossage RA, Klein Gebbink RJM et al (2000) J Am Chem Soc 122:12112–12124
20. Breinbauer R, Jacobsen EN (2000) Angew Chem Int Ed 39:3604–3607
21. Konsler R, Karl J, Jacobsen EN (1998) J Am Chem Soc 120:10780–10781
22. Zheng ZJ, Chen J, Li Y-S (2004) J Organomet Chem 689:3040–3045
23. Kassube JK, Wadepohl H, Gade LH (2009) Adv Synth Catal 35:607–616
24. Ooe M, Murata M, Mizugaki T et al (2004) J Am Chem Soc 126:1604–1605
25. (a) Ooe M, Murata M, Mizugaki et al (2002) Nano Lett 2:999–1002; (b) Scott RWJ, Datye AK, Crooks RM (2003) J Am Chem Soc 125:3708–3709
26. Yeung LK, Crooks RM (2001) Nano Lett 1:14–17
27. Reichardt C (1988) Solvents and solvent effects in organic chemistry, 2nd edn. Wiley, Weinheim
28. de Groot D, de Waal BFM, Reek JNH et al (2001) J Am Chem Soc 123:8453–8458
29. van de Coevering R, Alfers AP, Meeldijk JD et al (2006) J Am Chem Soc 128:12700–12713
30. Virboul MAN, Lutz M, Siegler MA et al (2009) Eur J Chem 15:9981–9986
31. Fujihara T, Obora Y, Tokunaga M et al (2005) Chem Commun 4526–4528
32. Wang HMJ, Lin IJB (1998) Organometallics 17:972–975
33. Oosterom GE, van Haaren RJ, Reek JNH et al (1999) Chem Commun 1119–1120
34. Oosterom GE, Steffens S, Reek JNH et al (2002) Top Catal 19:61–73
35. Bhyrappa P, Young JK, Moore JS et al (1996) J Am Chem Soc 118:5708–5711
36. Ohta H, Fujihara T, Tsuji Y (2008) Dalton Trans 379–385
37. Muller C, Ackerman LJ, Reek JNH et al (2004) J Am Chem Soc 126:14960–14963
38. Fujihara T, Yoshida S, Ohta H et al (2008) Angew Chem Int Ed 47:8310–8314
39. Snelders DJM, van Koten G, Klein Gebbink RJM (2009) J Am Chem Soc 131:11407–11416
40. Yamamoto K, Kawana Y, Tsuji M et al (2007) J Am Chem Soc 129:9256–9257
41. (a) Astruc D, Lu F, Azanzaes JR (2005) Angew Chem 117:8062–8083; (b) Wu L, Li Z-W, Zhang F et al (2008) Adv Synth Catal 350:846–862
42. Phan NTS, van der Sluys M, Jones CW (2006) Adv Synth Catal 348:609–679
43. (a) Allen DW, Taylor BF (1982) J Chem Soc Dalton Trans 51–54; (b) Andersen NG, Keay BA (2001) Chem Rev 101:997–1030
44. Kreiter R, Klein Gebbink RJM, van Koten G (2003) Tetrahedron 59:3989–3997
45. Snelders DJM, Kreiter R, Firet JJ et al (2008) Adv Synth Catal 350:262–266
46. (a) Weck M, Jones CW (2007) Inorg Chem 6:1865–1875; (b) Chen J, Vasiliev AN, Panarello AP et al (2007) Appl Catal A 325:76–86
47. (a) Hashiguchi S, Fujii A, Takehara J et al (1995) J Am Chem Soc 117:7562–7563; (b) Haack KJ, Hashiguchi Fujii A et al (1997) Angew Chem 109:297–300
48. Albrecht M, Hovestad NJ, Boersma J (2001) Eur J Chem 7:1289–1294
49. Janssen M, Müller C, Vogt D (2009) Adv Synth Cat 351:313–318